

# Structural Ordering and Symmetry Breaking in $\text{Cd}_2\text{Re}_2\text{O}_7$

J.P. Castellan,<sup>1</sup> B.D. Gaulin,<sup>1,4</sup> J. van Duijn,<sup>1</sup> M.J. Lewis,<sup>1</sup> M.D. Lumsden,<sup>2</sup> R. Jin,<sup>2</sup> J. He,<sup>3</sup> S.E. Nagler,<sup>2</sup> and D. Mandrus<sup>2,3</sup>

<sup>1</sup>Department of Physics and Astronomy, McMaster University, Hamilton, Ontario, L8S 4M1, Canada

<sup>2</sup>Solid State Division, Oak Ridge National Laboratory, P.O. Box 2008, Oak Ridge, TN, 37831 U.S.A.

<sup>3</sup>Department of Physics and Astronomy, The University of Tennessee, Knoxville, TN, 37996 U.S.A.

<sup>4</sup>Canadian Institute for Advanced Research, 180 Dundas St. W., Toronto, Ontario, M5G 1Z8, Canada

Single crystal X-ray diffraction measurements have been carried out on  $\text{Cd}_2\text{Re}_2\text{O}_7$  near and below the phase transition it exhibits at  $T_{C'} \sim 195$  K.  $\text{Cd}_2\text{Re}_2\text{O}_7$  was recently discovered as the first, and to date only, superconductor with the cubic pyrochlore structure. Superlattice Bragg peaks show an apparently continuous structural transition at  $T_{C'}$ , however the order parameter displays anomalously slow growth to  $\sim T_{C'}/10$ , and resolution limited critical-like scattering is seen above  $T_{C'}$ . High resolution measurements show the high temperature cubic Bragg peaks to split on entering the low temperature phase, indicating a (likely tetragonal) lowering of symmetry below  $T_{C'}$ .

PACS numbers: 61.10.-i, 64.70.Kb, 74.70.-b

Materials which crystallize into the cubic pyrochlore structure have been of intense recent interest, due to the presence of networks of corner-sharing tetrahedra within such structures [1]. Cubic pyrochlores display chemical composition  $\text{A}_2\text{B}_2\text{O}_7$ , and space group  $Fd\bar{3}m$ . Independently, both the A and B sublattices reside on networks of corner-sharing tetrahedra, an architecture also common to Laves phase cubic spinels, for example. Such materials have the potential to display phenomena related to geometrical frustration in the presence of anti-ferromagnetism. While much activity has focused on local magnetic moments in insulating pyrochlores, interesting metallic properties have also been observed recently. This has been the case, for example in  $\text{Nd}_2\text{Mo}_2\text{O}_7$  [2] where a large anomalous Hall effect has been measured, in  $\text{Cd}_2\text{Os}_2\text{O}_7$  where a metal insulator transition occurs near 226 K [3], as well as in the spinel  $\text{LiV}_2\text{O}_4$ , which is the only known transition metal based heavy fermion conductor [4].

While many metallic, cubic pyrochlore oxides exist, no superconductors were known to exist within this family of materials until very recently. Hanawa et al.[5], Sakai et al.[6], and Jin et al.[7] have all recently reported superconductivity in  $\text{Cd}_2\text{Re}_2\text{O}_7$ , the first such pyrochlore. The superconducting  $T_{Cs}$  are somewhat sample dependent and have been reported between 1 and 2 K. Moreover, the relatively high temperature metallic properties are anomalous, and may be driven by an as-yet poorly-understood phase transition near  $T_{C'} \sim 195$  K [8]. In this letter, we report on the nature of the phases above and below  $T_{C'}$  as well as the phase transition itself. We show compelling evidence for a splitting of the cubic Bragg peaks, indicating a lowering of symmetry below  $T_{C'}$ , likely to a tetragonal structure, as well as an unusual order parameter which grows very slowly with decreasing temperature.

$\text{Cd}_2\text{Re}_2\text{O}_7$  is a rather poor metal near room temper-

ature, exhibiting an almost flat resistivity between 200 K and 400 K [5, 6, 8]. Just below 200 K, the resistivity falls off sharply, continuing down to a low temperature Fermi liquid regime characterized by a  $T^2$  dependence to the resistivity between 2 K and roughly 60 K, and a residual resistivity on the order of  $10 \mu \text{ ohm}\cdot\text{cm}$  [5, 7]. On further lowering the temperature, the resistivity falls to zero, at  $T_C \sim 1.4$  K in crystals from the same batch as that under study here, indicating the onset of the superconducting state. Heat capacity measurements show a large anomaly at  $T_C$ , while above  $T_C$  these measurements give a Sommerfeld  $\gamma$  value of roughly  $30 \text{ mJ/mol}\cdot\text{K}^2$ . This result can be combined with A, the coefficient of the quadratic term in the temperature dependence of the resistivity, to give a Kadowaki-Woods ratio,  $A/\gamma$ , similar to that seen in highly correlated metals such as the heavy fermion superconductor  $\text{UBe}_{13}$  [7]. Recent transverse field  $\mu\text{SR}$  measurements [9] reveal the presence of a vortex lattice below  $T_C$ , with a large and temperature independent value of the penetration depth below  $0.4T_C$ . These measurements show  $\text{Cd}_2\text{Re}_2\text{O}_7$  to be a type II superconductor and are consistent with a nodeless superconducting energy gap.

Heat capacity measurements show a pronounced anomaly near  $T_{C'} \sim 200$  K, consistent with a continuous phase transition[8]. Electron diffraction from single crystals[8] and preliminary x-ray diffraction studies from powder samples[10] show the appearance of superlattice Bragg peaks at reflections such as  $(0,0,6)$  and  $(0,0,10)$ , which are inconsistent with the  $(0,0,h)$ :  $h=4n$  condition appropriate to the high temperature cubic space group. In addition, DC susceptibility measurements[5, 8] show an abrupt reduction in the susceptibility below  $T_{C'}$ , similar to that seen in magnetic singlet ground state systems, such as  $\text{CuGeO}_3$ [11] and  $\text{NaV}_2\text{O}_5$ [12].

The high quality single crystal used in the present study was grown as reported by He et al. [13]. It had

approximate dimensions  $4 \times 4 \times 2\text{mm}^3$  and a mosaic spread of less than  $0.04^\circ$  full width at half maximum. It was mounted in a Be can in the presence of a He exchange gas. The can was connected to the cold finger of a closed cycle refrigerator with approximate temperature stability of 0.005 K near  $T_{C'}$ , and 0.01 K elsewhere. X-ray diffraction measurements were performed in two modes, both employing an 18 kW rotating anode generator, Cu  $K\alpha$  radiation, and triple axis diffractometer. Relatively low resolution measurements of the superlattice Bragg peak intensities were obtained using a pyrolytic graphite (002) monochromator and a scintillation counter. Much higher resolution measurements were performed with a perfect Ge (111) monochromator, and a Bruker Hi Star area detector, mounted 0.75 m from the sample position on the scattered beam arm of the diffractometer. The high resolution experiment easily separated  $\text{Cu}_{K\alpha_1}$  from  $\text{Cu}_{K\alpha_2}$  diffraction, and was used for precision measurements of the lineshapes of both the principal and superlattice Bragg peaks.

Figure 1 shows the temperature dependence of the integrated intensity of low resolution scans of the (0,0,10) superlattice Bragg peak. Data was taken in separate warming and cooling runs, and is shown over an extended temperature range in the top panel, as well as over a narrow range near  $T_{C'}$  in the bottom panel. The form of this scattering, proportional to the square of the order parameter, is anomalous as it grows very slowly below  $T_{C'}$ , especially between  $\sim 170$  K and  $\sim 40$  K. A mean field phase transition displays the slowest growth among conventional models for cooperative behavior which exhibit continuous phase transitions. In Fig. 1, we compare the integrated intensity of the superlattice Bragg scattering to the square of the mean field order parameter[14], as well as to the square of the order parameter appropriate to the three dimensional Ising model[15]. Clearly the growth of the measured order parameter is much slower with decreasing temperature, than would be predicted by even mean field theory.

Closer to the phase transition, the measured order parameter does look more conventional as shown in the bottom panel of Fig. 1. This panel shows integrated intensity with both downward curvature below  $\sim 195$  K, and upward curvature above  $\sim 195$  K, consistent with the measurement of the order parameter squared below  $T_{C'}$ , and the measurement of fluctuations in the order parameter, or so-called critical scattering, above  $T_{C'}$ . Data in the temperature range 175 K to 190 K was analyzed assuming this to be the case, and fits were carried out in the approximate range of reduced temperature from 0.02 to 0.10, placing the data within a typical asymptotic critical regime. The fit of this data by the critical form:

$$\text{Intensity} = I_0 \left( \frac{T_{C'} - T}{T_{C'}} \right)^{2\beta} \quad (1)$$

is shown in the bottom panel of Fig. 1. The fit is of

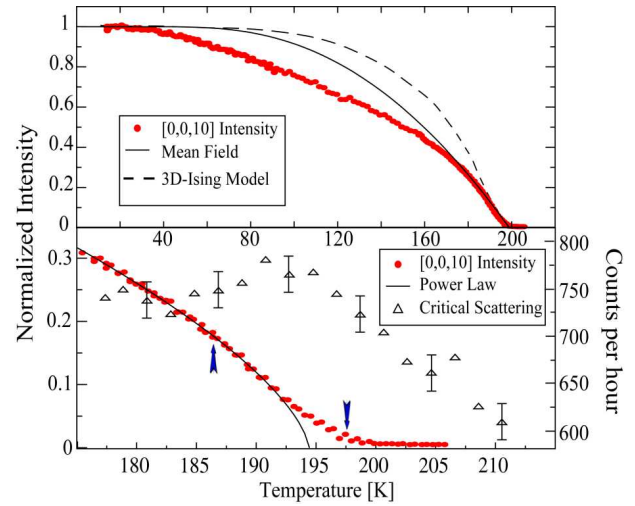


FIG. 1: The top panel shows the integrated intensity of the (0,0,10) superlattice Bragg peak as a function of temperature, compared with the square of the order parameter expected from mean field theory, and that expected from the 3 dimensional Ising model. The lower shows the same data in the immediate vicinity of  $T_{C'} \sim 194$  K, along with a fit to critical behavior modeled as a power law in reduced temperature (left-hand y-axis), and the broad critical scattering as measured at (0.04,0.064,10) (right-hand y-axis).

high quality, and it produces  $T_{C'} = 194.3 \pm 0.1$  K and a critical exponent  $\beta = 0.33 \pm 0.03$ , which is typical of three dimensional continuous phase transitions [16].

Although the (0,0,10) intensity above  $T_{C'} = 194.3$  appears to be critical scattering, we show below that it is anomalous and remains resolution limited at all temperatures measured.  $\mathbf{Q}$ -broadened critical fluctuations can be measured by moving slightly off the (0,0,10) Bragg position, however it is extremely weak. Scattering at (0.04,0.064,10) is shown in the bottom panel of Fig. 1 and it displays a weak peak near  $T_{C'}$ , as expected for a continuous phase transition. This broad scattering is measured in counts per *hour*, and it makes a negligible contribution to the overall scattering around (0,0,10) above  $T_{C'} = 194.3$ . It does however provide a consistency check on the phase transition occurring at 194.3 K.

High resolution measurements of the lineshape of the (0,0,10) superlattice Bragg peak, shown in Fig. 2, reveal that almost all of the this scattering above  $T_{C'} = 194.3$  K remains resolution limited; it is indistinguishable from the superlattice scattering below 194.3 K, albeit weaker in intensity. Figure 2 shows maps of the scattering at and around the (0,0,10) superlattice position at temperatures of 185.7 K and 197.4 K. As indicated by the arrows superposed on the order parameter shown in the bottom panel of Fig. 1, these temperatures correspond to well below and well above  $T_{C'}$ .

The 197.4 K data set definitely falls within the upward curvature regime of the temperature dependence of the

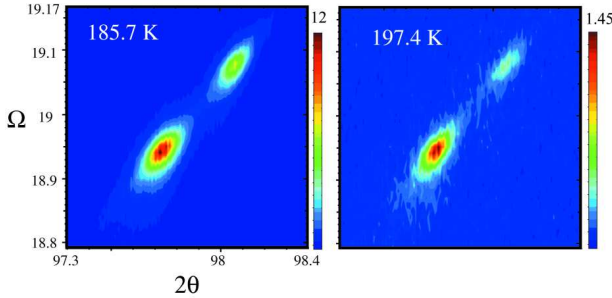


FIG. 2: High resolution scans of the scattering at and near the  $(0,0,10)$  superlattice Bragg peak positions are shown for the temperatures marked by arrows in the inset to Fig. 1. These temperatures correspond to well below and well above  $T_{C'}$ . Data is shown in maps as a function of sample rotation angle  $\Omega$  and scattering angle  $2\theta$ . The two diffraction features at  $2\theta$  values of  $\sim 97.7^\circ$  and  $98.07^\circ$  are from  $\text{Cu K}_{\alpha 1}$  and  $\text{Cu K}_{\alpha 2}$  radiation, respectively. The top of the linear color scale is different for each data set. It is clear that the lineshape does *not* broaden appreciably on passing through  $T_{C'}$ .

superlattice integrated intensity, and would normally be expected to be due to fluctuations in the order parameter rather than due to the order parameter itself. As discussed above, such critical scattering is expected to broaden in  $\mathbf{Q}$ , and therefore in angular coordinates, as the temperature increases beyond  $T_{C'}$ , indicating a finite and decreasing correlation length. Such broadening is clearly not observed in this scattering above  $T_{C'}$ .

The anomalous nature of the lineshape of the superlattice scattering above  $T_{C'}$  may be due to “second length scale” scattering[17], which has often been observed in high resolution synchrotron x-ray experiments near phase transitions in crystalline materials. It is not fully understood, but has been associated with the effect of near-surface quenched disorder on the phase transition. The x-rays in the present measurements have a penetration depth of the order of ten microns (tens of thousands of unit cells) and are thus not particularly surface sensitive.

It may also be that this superlattice Bragg scattering is not the primary order parameter for the phase transition near  $T_{C'}$ , but is a secondary feature, pulled along by the true underlying phase transition. The anomalously slow growth of the  $(0,0,10)$  superlattice Bragg peak at low temperatures also supports such an interpretation.

We also carried out measurements of the principal Bragg peaks (which satisfy the  $(00h)$ :  $h=4n$  relation) at high scattering angle and in high resolution mode. Scans along the longitudinal direction, cutting through both  $\text{Cu K}_{\alpha 1}$  and  $\text{Cu K}_{\alpha 2}$  peaks of the  $(0,0,12)$  principal Bragg peaks, are shown in the right hand panels of Fig. 3 on a linear scale, and in the bottom, left panel of Fig. 3 on a semi-log scale. For comparison, similar longitudinal scans through the superlattice  $(0,0,10)$  Bragg peaks are shown on a semi-log scale in the top left panel of Fig.

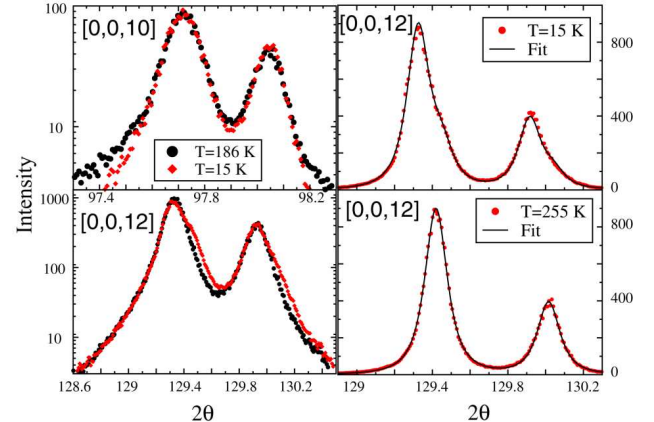


FIG. 3: The right hand panels shows longitudinal cuts taken through the  $(0,0,12)$  principal Bragg peak position well above  $T_{C'}$  (bottom) and well below (top). This data, on a linear scale, shows a clear shoulder on the high  $2\theta$  side of both the  $\text{Cu K}_{\alpha 1}$  and  $\text{K}_{\alpha 2}$  peaks. The left hand panels show the superlattice  $(0,0,10)$  (top) and principal  $(0,0,12)$  (bottom) Bragg peaks on a semi-log scale, at temperatures just below and well below  $T_{C'}$ . Clearly, while the principal Bragg peaks split on lowering the temperature, the superlattice peaks do not.

3. The data sets at the two temperature which make up both semi-log plots on the left side of Fig. 3 have been shifted slightly in  $2\theta$  and, in the case of  $(0,0,10)$ , scaled in intensity to allow for comparison.

A shoulder is clearly seen to develop on the high angle side of the  $(0,0,12)$  peaks as the temperature is lowered below  $T_{C'}$ . This indicates a splitting of the cubic Bragg peak into a lineshape characterized by at least two different lattice parameters, and consequently a symmetry lower than cubic, likely tetragonal, in the low temperature state below  $T_{C'} \sim 194.3$  K.

A similar splitting of the  $(0,0,10)$  superlattice Bragg peak is *not* observed. The superlattice Bragg peaks do not exist above  $T_{C'}$  and thus we must compare superlattice data taken below, but near  $T_{C'}$  with that taken well below  $T_{C'}$ . That is what is shown for both the principal  $(0,0,12)$  Bragg peak and the superlattice  $(0,0,10)$  Bragg peak at temperatures of 186 K and 15 K, respectively in the left hand panels of Fig. 3. At 186 K, the splitting is not yet evident in either the principal,  $(0,0,12)$ , or superlattice,  $(0,0,10)$ , Bragg peaks, but by 15 K it is clear in the principal Bragg peak, but not in the superlattice Bragg peaks.

We fit the high temperature data at  $(0,0,12)$  to a phenomenological form at 255 K, assuming this to be the resolution-limited lineshape. We then fit  $(0,0,12)$  data at all temperatures to a form assuming the superposition of two such lineshapes, displaced from each other in scattering angle ( $2\theta$ ). This protocol allowed us to extract peak positions for each of two peaks, giving the lattice parameters as a function of temperature. This analysis assumes that only two lattice parameters are present at low tem-

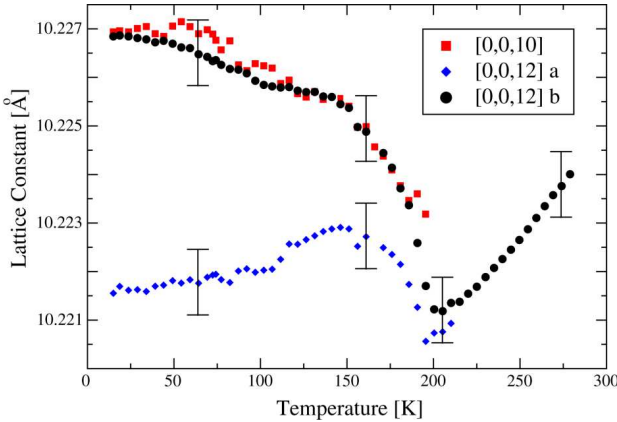


FIG. 4: The temperature dependence of the lattice parameters extracted from fits to the (0,0,12) principal Bragg peaks (shown as solid lines in Fig. 3) are shown, along the temperature dependence of the superlattice (0,0,10) Bragg peak periodicity below  $T_{C'}$ .

peratures, that is that the low temperature structure is tetragonal. The data at 15 K in the top right panel of Fig. 3 shows the quality of this fit, and clearly the description of the data is very good. The resulting tetragonal lattice parameters as a function of temperature are shown in Fig. 4.

The behavior of the lattice parameters as a function of temperature is striking. The cubic lattice parameter displays the usual thermal contraction with decreasing temperature until near  $T_{C'}$ . The splitting in the lattice parameters first develops near 200 K, with a 30 K interval from  $\sim 190$  K to 160 K in which both lattice parameters increase with decreasing temperature. This trend continues to lower temperatures for the larger of the two lattice parameters, while the smaller turns over below  $\sim 150$  K and displays relatively weak contraction to lower temperatures. At the lowest temperature measured, 15 K, the maximum splitting in lattice parameter measured is about 0.005 Å or 0.05 %.

The (0,0,10) superlattice peak does not show any splitting, and the temperature dependence associated with its periodicity is also shown in Fig. 4. It clearly follows the upper branch of the two lattice parameters associated with (0,0,12). These results imply that the low temperature state below  $T_{C'}$  is likely twinned tetragonal, such that two of (0,0,12), (0,12,0) and (12,0,0) have one lattice parameter, while the other has a slightly different one. The fact that the superlattice peak displays no splitting implies that only the subset of (0,0,10), (0,10,0) and (10,0,0) which follow the upper branch of the lattice parameter vs temperature curve shown in Fig. 4, exists. The other(s) is (are) systematically absent.

These observations allow us to discuss possible tetragonal space groups appropriate to the low temperature state below  $T_{C'}$ . As the transition appears to be close to continuous, we assume the low temperature state to be

a gradual distortion of the high temperature cubic state, and thus the low temperature space group should be a subgroup of  $Fd\bar{3}m$ . There are two body-centered subgroups of  $Fd\bar{3}m$  which, in the presence of twinning, would split (0,0,12) and allow a single periodicity for (0,0,10). These are  $I4_1$  and  $I4_122$ . In both cases the primitive unit vectors of the basal ( $a'-a'$ ) plane are rotated by 45° relative to the unit vectors,  $a$ , of the high temperature cubic unit cell, and  $a'=a/\sqrt{2}$ .

While we cannot be more precise as to the low temperature space group at this time, we have unambiguously shown the symmetry of the low temperature state to be lower than cubic, and that this cubic symmetry breaking is an essential feature of the phase transition. The most likely scenario is a cubic-tetragonal phase transition, with the primary order parameter being the difference in lattice parameters, given by  $\sqrt{2}a'-a$ . Finally we note that we do not expect this splitting of the lattice parameters to be evident in bulk measurements, such as dilatometry, unless a single domain sample can be produced at low temperatures.

We wish to acknowledge useful discussions with J.F. Britten. This work was supported by NSERC of Canada. Oak Ridge National Laboratory is managed by UT-Battelle, LLC the U.S. D.O.E. under Contract DE-AC05-00OR22725. Work at UT is supported by NSF DMR-0072998.

- 
- [1] for recent reviews see: S.T. Bramwell and M.J.P. Gingras, *Science*, **294**, 1495 (2001), **Magnetic Systems with Competing Interactions**, edited by H.T. Diep (World Scientific, Singapore (1994).
  - [2] Y. Taguchi et al., *Science*, **291**, 2573 (2001).
  - [3] D. Mandrus et al., *Phys. Rev. B*, **63**, 195104 (2001).
  - [4] S. Kondo et al., *Phys. Rev. Lett.*, **78**, 3729, (1997); C. Urano et al., *Phys. Rev. Lett.*, **85**, 1052 (2000).
  - [5] M. Hanawa et al., *Phys. Rev. Lett.*, **87**, 187001, (2001)
  - [6] H. Sakai et al., *J. Phys. Cond. Mat.* **13**, L785 (2001).
  - [7] R. Jin et al., *Phys. Rev. B*, **64**, 180503(R), (2001)
  - [8] R. Jin et al., cond-mat/0108402.
  - [9] M.D. Lumsden et al., cond-mat/0111187; R. Kadono et al., cond-mat/0112448.
  - [10] M. Hanawa et al., cond-mat/0109050.
  - [11] M. Hase, I. Terasaki, and K. Uchinokura, *Phys. Rev. Lett.* **70**, 3651 (1993).
  - [12] M. Isobe and Y. Ueda, *J. Phys. Soc. Jpn.* **65**, 1178 (1996).
  - [13] J. He et al., unpublished.
  - [14] for example: M. Plischke and B. Bergerson, *Equilibrium Statistical Physics, 2nd Edition*, World Scientific Press (1994).
  - [15] D.M. Burley, *Philos. Mag.* **5**, 909 (1960).
  - [16] M.F. Collins, *Magnetic Critical Scattering*, Oxford University Press (1989).
  - [17] for example: S.R. Andrews, *J. Phys. C* **19**, 3721 (1986).; T.R. Thurston et al, *Phys. Rev. Lett.* **70**, 3151 (1993).